Available online at www.sciencedirect.com
ScienceDirect
Ceramics International 35 (2009) 2249–2254
CERAMICS INTERNATIONAL
www.elsevier.com/locate/ceramint

Manufacturing of highly porous calcium phosphate bioceramics via gel-casting using agarose

Marek Potoczek [a,*], Aneta Zima [b], Zofia Paszkiewicz [b], Anna Ślósarczyk [b]

[a] *Rzeszow University of Technology, Faculty of Chemistry, ul. W.Pola 2, 35-959 Rzeszow, Poland*
[b] *UST – University of Science and Technology, Faculty of Materials Science and Ceramics, Department of Ceramics and Refractory Materials, Al. Mickiewicza 30, 30-059 Krakow, Poland*

Received 22 October 2008; received in revised form 10 November 2008; accepted 27 December 2008
Available online 22 January 2009

Abstract

There is a technological need for highly porous bioceramics to be produced in an environmentally friendly manner. Gel-casting of highly porous HAp-(α-TCP) (CaP) foams using agarose as a gelling agent was investigated. Foaming of gel-cast suspension was performed at the temperature of 60 °C followed by transformation of the foams from a liquid state to a gelled state by cooling them to 15 °C. The sintered (1250 °C, 2 h soaking time) foams were characterized by X-ray diffraction (XRD), scanning electron microscopy (SEM), N_2 adsorption isoterm and Hg porosimetry. XRD study revealed that additives used in the gel-casting process did not influence the phase composition of the investigated materials. The macroporous microstructure of HAp-(α-TCP) foams was typically composed of approximately spherical pores (cells) interconnected by circular windows. The foams exhibited a broad pore size distribution with cells and windows ranging from 250 to 900 μm, and from 25 to 250 μm, respectively. The mode for spherical pore size was approximately 500 μm while the above value for window was ∼100 μm. Additionally, the small amount of wall microporosity in the range of 0.2–0.9 μm was confirmed by SEM and Hg porosimetry. The obtained porous (P = 90%) HAp-(α-TCP) scaffolds with interesting two types of macropores and a small amount of micropores seem to be a promising bone substitution material.

Keywords: B. Porosity; D. Apatite; Bioceramics; Gel-casting

1. Introduction

1.1. Porous hydroxyapatite ceramics

Over the past decades, hydroxyapatite [$Ca_{10}(PO_4)_6(OH)_2$] (HAp) and related calcium phosphates (CaPs) have been widely used as implant materials due to close similarity of their composition to inorganic phase of natural bone and high biocompatibility. Hydroxyapatite bioceramics are applied both, in dense and porous forms. Surface area of porous bodies is much higher which guarantees good fixation and allows more cells or tissue to be carried by the implant in comparison with dense HAp. For bone ingrowth, pore size greater than 100 μm but less than 400 μm is considered to be optimum. However, in the literature there are contradictory reports concerning bone ingrowth in pores below 100 μm and above 500 μm [1–3]. Another important factor is the dimension of the window between the interconnected cells as the small one can prevent osteoconduction through the scaffold structure. The optimum size of the windows should be about 100 μm [4].

A number of techniques have been developed for producing porous bioceramics, including incorporation of pore-creating additives [5,6], replication of polymer foams by impregnation [7], dual-phase mixing technique [8], freeze casting method [9], and the foaming of gel-casting suspensions [10]. According to Jones and Hench [11], gel-casting technique is the method resulting in the production of scaffolds most closely mimicking the structure of trabecular bone. Moreover, the sintered gel-cast foams due to their well-densified struts show relatively high mechanical strength [10].

1.2. Preparation of porous implants by gel-casting method

Gel-casting of porous materials has been developed as a result of the combination of the gel-casting process and

* Corresponding author. Tel.: +48 17 8651749; fax: +48 17 8543655.
E-mail address: potoczek@prz.edu.pl (M. Potoczek).

0272-8842/$34.00
doi:10.1016/j.ceramint.2008.12.006

the aeration of the ceramic suspensions containing both, foaming and gelling agents [12]. The *in situ* polymerisation of organic monomers, as gelling agents, leads to fast solidification, resulting in highly porous and relatively strong bodies, which could withstand machining. The obtained ceramic foams consist of interconnected porous network of spherical cells.

In the early gel-casting systems, acrylamide monomers were used as gelling agents for the preparation of HAp foams [10]. In order to avoid the health hazard problems with monomers, other gelling systems were applied for gel-casting of hydroxyapatite porous implants. Polymers, such as: polyfunctional epoxy compound crosslinked by polyethyleneimine [13], modified or naturally occurring biopolymers, such as methyl cellulose [14,15], albumin [16], starch [17] and agarose [18] have been used.

In our former studies based on commercial HAp powders, we proposed to use agarose as a gelling agent [18]. In the present investigations, hydroxyapatite of very high chemical purity having medical attest was applied [19]. The initial medical grade HAp powder synthesized by the wet method at UST was used to prepare the suspensions designed for manufacturing of highly porous implant materials. The aim of our work was to prepare and characterize CaP scaffolds obtained via gel-casting. Special attention was paid to the pore size distribution and the type of connections (i.e. windows) between the spherical pores present in the studied materials. The above parameters are very important since they determine mechanical strength of implants and possibility of their biological fixation (i.e. creation of direct bonding with natural bone).

2. Materials and methods

2.1. Preparation and characterization of initial HAp powders

Hydroxyapatite powder was synthesized by the precipitation method by the reaction of an aqueous slurry of $Ca(OH)_2$ with a solution of H_3PO_4, as previously described [19,20]. CaO (p.a.) was initially calcined at 900 °C. In the process of preparing a $Ca(OH)_2$ suspension, CaO was added to distilled water and stirred for 30 min. 0.5 M $Ca(OH)_2$ suspension in 1000 ml distilled water was used to the synthesis. A solution of 0.3 M H_3PO_4 in 1000 ml distilled was prepared. The solution was slowly added to $Ca(OH)_2$ suspension at the rate of 17 ml/min. The reaction mixtures were vigorously stirred during the precipitation process, which was performed in the temperature range 23–25 °C. During powder precipitation, the ammonium solution was added in such a way to maintain pH 11 until the end of the process. The resulting precipitate was washed with distilled water, dried at 90 °C, ground in a rotating/vibrating mill and then calcined at 800 °C.

HAp thus produced contained isometric agglomerates of particles (Fig. 1). Its specific surface area measured by BET method was equal to 15.2 $m^2\,g^{-1}$. The helium density was 3.05 g cm^{-3}.

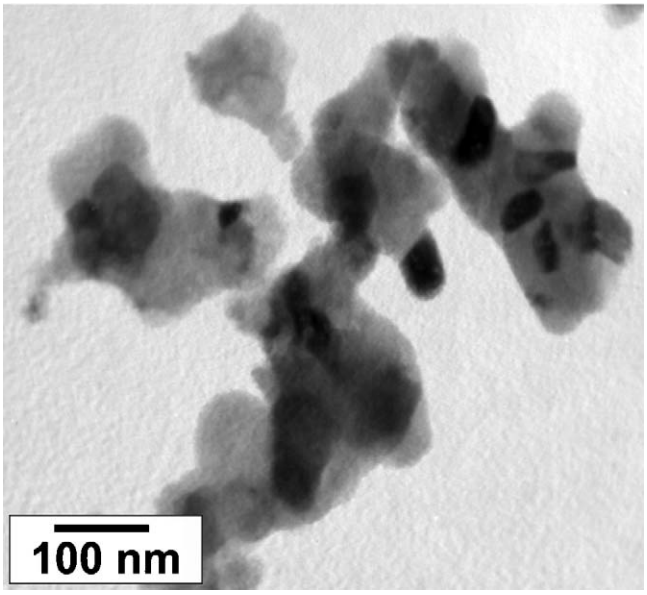

Fig. 1. TEM micrograph of initial HAp powder.

2.2. Preparation of highly porous HAp foams via gel-casting technique

Ceramic suspensions with a high amount of HAp powder as a solid phase (49 vol.%) were prepared by adding 0.64 mass% of dispersant (Darvan 811, R.T. Vanderbilt, U.S.A.). Their homogenisation was carried out by ball milling using alumina balls and jar. Agarose solutions (2.5 mass%) were prepared by mixing agarose powder (POCH, Gliwice, Poland, Cat. No. 111720491) with distilled water followed by heating for 11 min in an autoclave at 121 °C and 1.4 bar. The 2.5 mass% agarose solution was added to the HAp slurry maintaining the temperature at 60 °C. The final HAp content was fixed at 32 vol.%. Total concentration of active gelling matter in the final slurry was equal to be 0.9 mass% as dry HAp, which corresponded to 1.3 mass% of agarose with respect to water.

Foaming was carried out at 60 °C through agitation using a double-blade mixer. Details of the developed foaming process resulting in the preparation of highly porous (∼90%) ceramics were described in our earlier work [21]. Addition of non-ionic surfactants (Tergitol TMN-10, Aldrich, Germany and Simulsol SL-26, Seppic, France) was necessary to stabilize the foams. The concentration of each surfactant was 0.34 g/100 ml of slurry. The foamed suspension containing agarose was poured into a mould. The mould was cooled by water (15 °C) to transform the foam from a liquid state to a gelled state. The green bodies were then de-moulded and dried at room temperature. Sintering was performed at 1250 °C for 2 h at a heating rate of 2 °C min^{-1} to 600 °C and then 4 °C min^{-1} up to the sintering temperature. The samples were cooled to 900 °C at a cooling rate the rate of 4 °C min^{-1}, and then furnace cooled.

2.3. Characterization

Phase composition of raw powders and sintered ceramics was identified by X-ray diffraction analysis. XRD measure-

ments were performed using monochromatic Cu Kα radiation within the 2θ range of 20–60° with the scan rate of 0.008° s^{-1}. The phase quantification was made by the Rietveld method using the program X'Pert Plus.

Helium density of raw powders and sintered foams was determined by helium picnometer (AccuPyc 1330). Apparent density of investigated bodies was calculated from the mass and dimensions of minimum five samples having regular shapes. Total porosity (P) was evaluated based on the helium and the apparent densities according to Eq. (1):

$$P\,(\%) = \frac{\rho_s - \rho_a}{\rho_s} \times 100 \quad (1)$$

where ρ_s and ρ_a are the helium density (g cm^{-3}) and the apparent density (g cm^{-3}), respectively.

Specific surface area of raw powders and sintered foams was measured by BET technique, using nitrogen (ASAP 2000, Micrometric).

Microstructure of ceramic foams was examined by scanning electron microscopy (Jeol JSM-5500 LV). SEM pictures for monitoring cellular microstructure of the sinters were analyzed in terms of estimation of cell sizes (spherical pores) and window sizes (interconnected pores). This allowed window and cell size to be estimated from the cells which presented an equator in the fracture surface and from the windows by taking the major axis of oblique windows as their diameter. The diameter of minimum 250 cells and 350 windows were measured and the cell and window size distributions were calculated.

Pore size distribution (0.009–360 μm) of the sintered scaffolds was determined using mercury intrusion porosimetry (Autopore II 9220, Micrometric). This allowed for measurements of microporosity within spherical pore walls, as well as for the evaluation of interconnected macropore size distribution (windows).

Compressive and flexural strengths of scaffolds were measured using an Instron testing machine (Model: 3345). Flexural strength was determined in a three point bending tests. The bars with dimensions of 50 mm × 10 mm × 5 mm were used and the span was 20 mm. The crosshead speed was 2.0 mm min^{-1} for all tested samples. Compressive strength was determined in uni-axial compression tests, using 2.0 mm min^{-1} crosshead speed. The samples in the form of rectangular bars with dimensions of 8 mm × 8 mm × 16 mm were used. The loaded surfaces were covered with a thin sponge layer to obtain uniform load distribution throughout the faces. In all mechanical determinations, results were based on average of 20 samples.

3. Results and discussion

3.1. Phase composition

X-ray results for HAp powders initial and fired at 1250 °C and HAp scaffold after sintering at 1250 °C are presented in Fig. 2. The pattern of initial powder showed only the characteristic reflections of HAp (Fig. 2a). After heat treatment at 1250 °C the sample was consisted of hydroxyapatite as the dominant phase (93.1 mass%) and several percent (7.9 mass%) of α-$Ca_3(PO_4)_2$ (α-TCP) as the secondary phase (Fig. 2b). No other phases, such as β-TCP or CaO were observed. The same phases were present when gel-cast scaffold was heated at 1250 °C (Fig. 2c). This confirmed that additives used in the gel-casting process (slurry dispersant, foaming and gelling agents) did not influence the phase composition of the investigated material.

3.2. Physical properties

Shrinkage after sintering of porous samples was 18%. Their helium and apparent densities were 3.03 and 0.31 g cm^{-3}, respectively. The calculated total porosity of the obtained body was 89.8%, while the specific surface area was 0.24 m^2 g^{-1}.

3.3. Microstructure and pore size distribution

The microstructure of the sintered foams is presented in Fig. 3. The obtained scaffolds were typically composed of approximately spherical cells interconnected by circular windows (Fig. 3a). Spherical pores were associated with densified polycrystalline struts (Fig. 3b). The presence of densified struts is the main microstructure difference between the gel-casting technique and another method, known as a replication process. One of the drawbacks of the replication process is the tendency to leave hollow struts, causing lowering of the mechanical properties.

The grain microstructure of the spherical pore wall is presented in Fig. 3c. The grain size was approximately 2 μm. Small wall micropores (less than 1 μm) were visible. Several studies [22,23] suggest that microporosity improves bone growth into scaffolds.

Size distributions of spherical and interconnected (window) pores are presented in Figs. 4 and 5 by histograms obtained from the results of image analysis of SEM micrographs. The

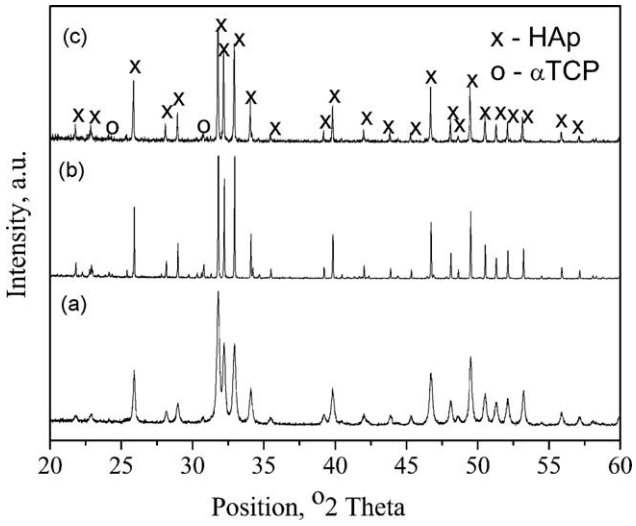

Fig. 2. X-ray diffraction patterns of the samples: (a) initial HAp powder, (b) HAp-(α-TCP) powder after sintering at 1250 °C, and (c) gel-cast scaffold after sintering at 1250 °C.

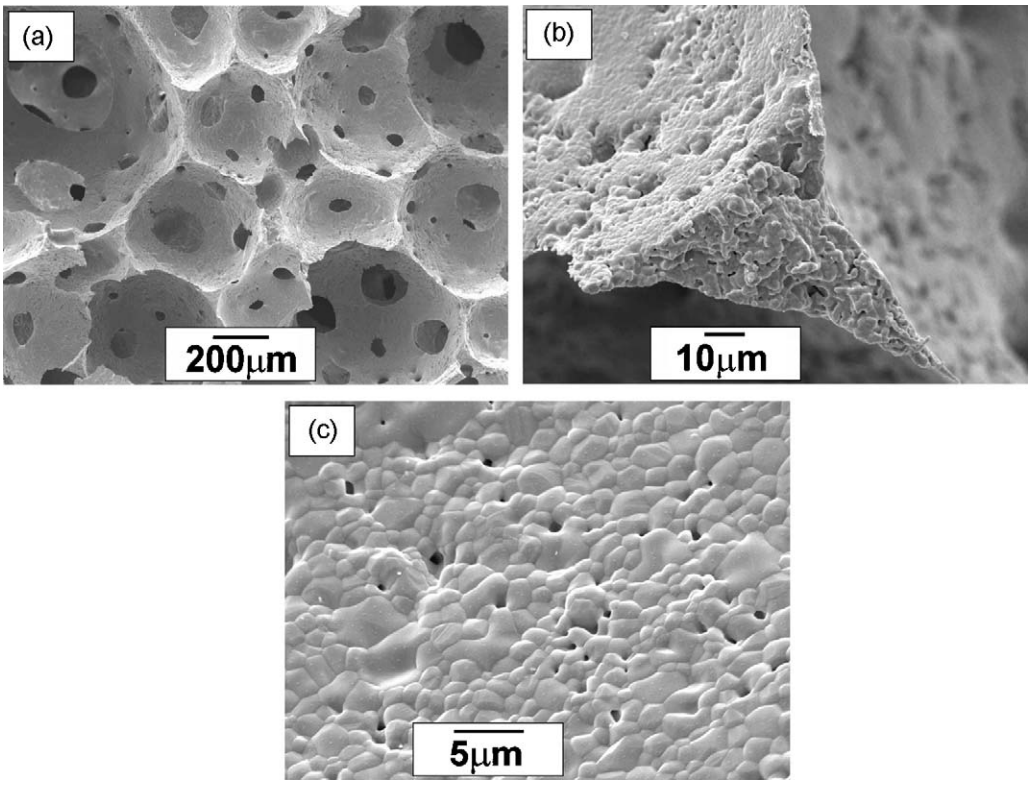

Fig. 3. SEM micrographs of the sintered CaP foams: (a) cross-section of the foam, (b) cross-section of the strut, and (c) microstructure of the spherical pore wall.

foams exhibited a broad pore size distribution with spherical cells and windows ranging from 250 to 900 μm, and from 25 to 250 μm, respectively. The mode was approximately 500 μm for cells and approximately 100 μm for windows.

Fig. 6 is a mercury intrusion curve for the CaP sintered foam. As can be seen from Fig. 6, scaffold porosity is determined by a small amount of wall micropores in the range of 0.2–0.9 μm and a large amount of inter-pore connections (windows) ranging from 20 to 300 μm with the mode diameter of 154 μm. This value was greater than that obtained by image analysis of SEM micrographs. However, comparison of the results obtained by both techniques is difficult since their approach is different. Image analysis measures all available stereographic diameters, whereas the entire pore size distribution is detected via mercury porosimetry. In addition, mercury porosimetry can underestimate the actual pore size due to the ''ink bottle effect''. Nevertheless, the interconnected window size obtained by two above techniques was greater than 100 μm. This range is sufficient for maintaining cell penetration and tissue formation in the scaffold.

3.4. Mechanical strength

Figs. 7 and 8 are typical examples of compressive stress–strain curve and flexural stress–strain curve for the ceramic

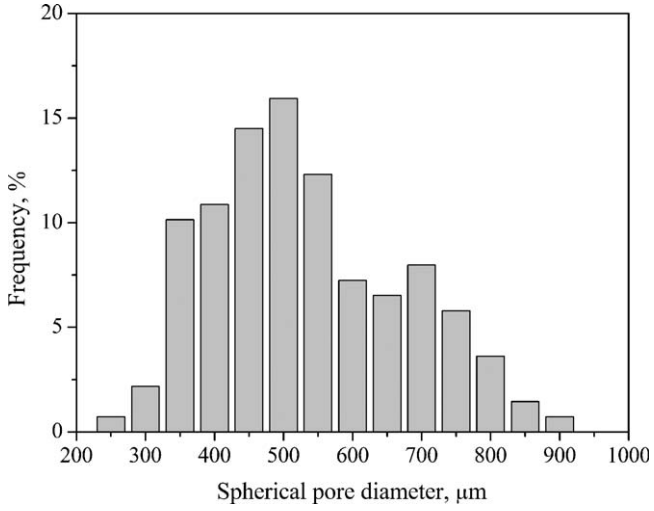

Fig. 4. Cell size distribution of the CaP foam.

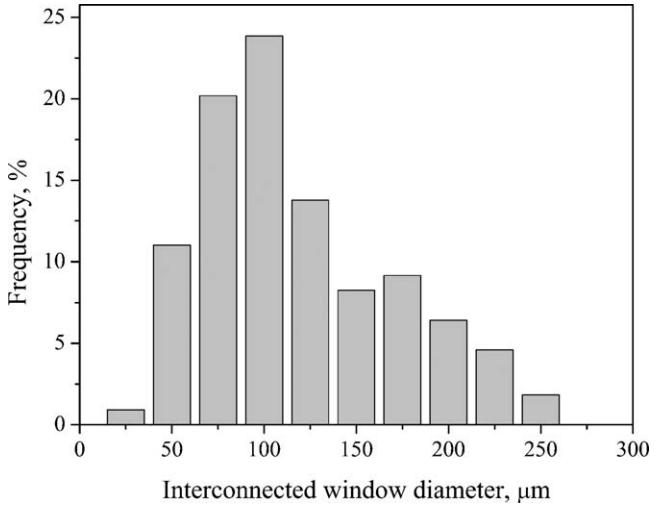

Fig. 5. Window size distribution of the CaP foam.

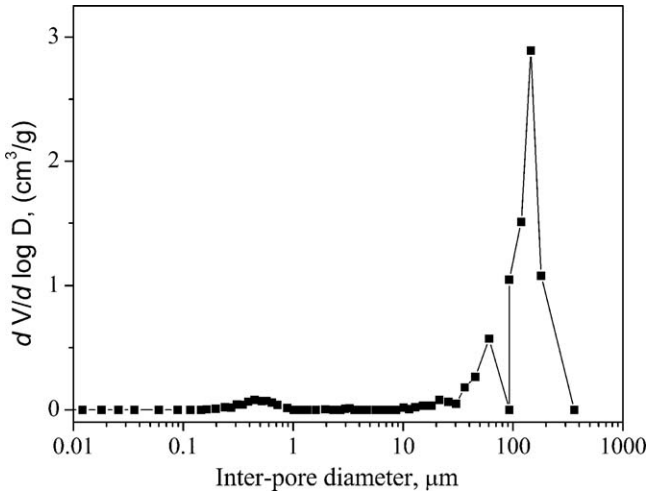

Fig. 6. Pore size distribution curve of the CaP foam measured by Hg porosimeter.

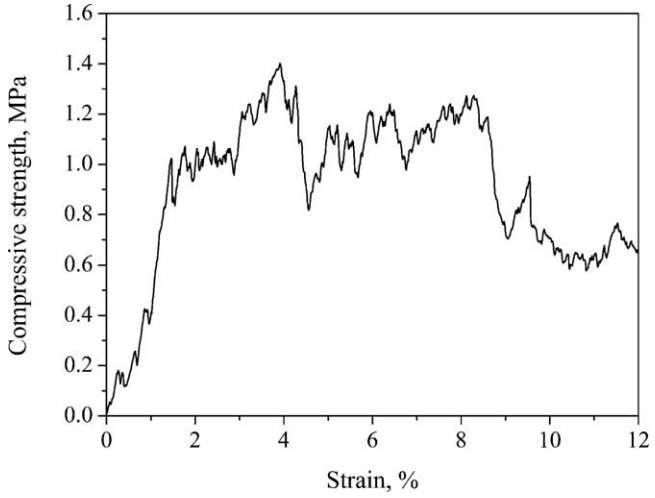

Fig. 7. Typical compressive stress–strain curve of the CaP foam.

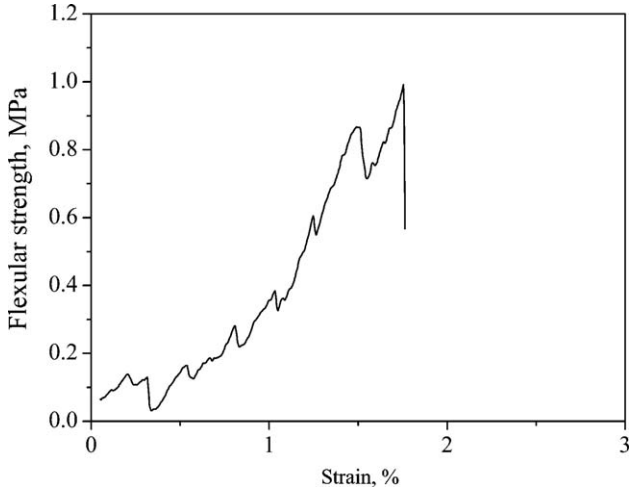

Fig. 8. Typical flexural stress–strain curve of the CaP foam.

foams with porosity level of 90%. The compressive stress–strain plot shows a typical behaviour for ceramic foams, i.e. subsequent brittle crushing and densification following the fracture [24]. The mean value of compressive strength was 0.99 ± 0.49 MPa, while the mean value of flexural strength was 0.93 ± 0.23 MPa. The minimum and maximum compressive strengths was 0.44 and 1.92 MPa, respectively. The flexural strengths varied between 0.59 and 1.40 MPa.

As it is generally known, compressive strength is much higher than that of flexural strength for dense ceramic materials. However, the resulting compressive and flexural strengths were almost same due to the low mechanical strengths. This can be explained by Gibson and Ashby model [25], i.e. collapse of highly porous brittle foams occurs as a flexural rupture mode and is determined by the modulus of rupture of strut not by the compressive strength of strut.

The obtained mechanical strengths are not sufficient for load-bearing part of bone implants. Nevertheless, the applied gel-casting technique resulted in highly porous materials with better mechanical strength than that obtained by other routes [24]. It was probably caused by the spherical shape of large pores associated with a densified polycrystalline matrix of the material walls.

4. Conclusion

The usefulness of gel-casting technique applying an environmentally friendly gelling agent (agarose) in manufacturing of highly porous HAp-(α-TCP) bioceramics was discussed. The additives used in the gel-casting process did not influence the phase composition of the investigated material. The obtained porous ($P = 90\%$) CaP scaffold had macropores (spherical ~500 μm and interconnecting windows ~100 μm in diameter) and a small amount of micropores (0.2–0.9 μm), being a promising bone substitution material. Further biological studies are however necessary, before actual applications.

Acknowledgement

This work has been supported by the Polish Ministry of Science and Higher Education. Project No. R 15 003 03.

References

[1] O. Gauthier, J.M. Bouler, E. Aguado, P. Pilet, G. Daculsi, Macroporous biphasic calcium phosphate ceramics: influence of macropore diameter and macroporosity percentage on bone ingrowth, Biomaterials 19 (1–3) (1998) 133–139.
[2] K.A. Hing, S.M. Best, W. Bonfield, Characterization of porous hydroxyapatite, J. Mater. Sci. Mater. Med. 10 (3) (1999) 135–145.
[3] A.G. Mikos, G. Sarakinos, M.D. Lyman, D.E. Ingber, J.P. Vacanti, P. Langerr, Prevascularization of porous biodegradable polymers, Biotechnol. Bioeng. 42 (6) (1993) 716–723.
[4] B.S. Chang, C.K. Lee, K.S. Hong, H.J. Youn, H.S. Ryu, S.S. Chung, K. Park, Osteoconduction at porous hydroxyapatite with various pore configurations, Biomaterials 21 (12) (2000) 1291–1298.
[5] T. Livingston, P. Ducheyne, J. Garino, In vivo evaluation of a bioactive scaffold for bone tissue engineering, J. Biomed. Mater. Res. 62 (2002) 1–13.

[6] J. Szymura-Oleksiak, A. Ślósarczyk, A. Cios, B. Mycek, Z. Paszkiewicz, S. Szklarczyk, D. Stankiewicz, The kinetics of pentoxifylline release *in vivo* from drug-loaded hydroxyapatite implants, Ceram. Int. 27 (2001) 767–772.
[7] S. Callcut, J.C. Knowles, Correlation between structure and compressive strength in a reticulated glass-reinforced hydroxyapatite foam, J. Mater. Sci. Mater. Med. 13 (2002) 485–489.
[8] S.H. Li, J.R. De Wijn, P. Layrolle, K. de Groot, Synthesis of macroporous hydroxyapatite scaffolds for bone tissue engineering, J. Biomed. Mater. Res. 61 (2002) 109.
[9] E.J. Lee, Y.H. Koh, B.H. Yoon, H.E. Kim, H.W. Kim, Highly porous hydroxyapatite bioceramics with interconnected pore channels using camphene-based freeze casting, Mater. Lett. 61 (2007) 2270–2273.
[10] P. Sepulveda, F.S. Ortega, M.D.M. Innocentini, V.C. Pandolfelli, Properties of highly porous hydroxyapatite obtained by the gelcasting of foams, J. Am. Ceram. Soc. 83 (12) (2000) 3021–3024.
[11] J.R. Jones, L.L. Hench, Regeneration of trabecular bone using porous ceramics, Curr. Opin. Solid State Mater. Sci. 7 (2003) 301–307.
[12] P. Sepulveda, J.G.P. Binner, Processing of celluar ceramics by foaming and *in situ* polymerization of monomers, J. Eur. Ceram. Soc. 19 (1999) 2059–2066.
[13] N. Tamai, A. Myoui, T. Tomita, T. Nakase, J. Tanaka, T. Ochi, H. Yoshikava, Novel hydroxyapatite ceramics with an interconnective porous structure exhibit superior osteoconduction *in vivo*, J. Biomed. Mater. Res. 59 (1) (2002) 110–117.
[14] L.A. Cyster, D.M. Grant, S.M. Howdle, F.R.A.J. Rose, D.J. Irvine, D. Freeman, C.A. Scotchford, K.M. Shakesheff, The influence of dispersant concentration on the pore morphology of hydroxyapatite ceramics for bone tissue engineering, Biomaterials 26 (2005) 697–702.
[15] N.O. Engin, A.C. Tas, Manufacture of macroporous calcium hydroxyapatite bioceramics, J. Eur. Ceram. Soc. 19 (1999) 2569–2572.
[16] A.F. Lemos, J.M.F. Ferreira, The valence of egg white for designing smart porous biomaterials: as foaming and consolidation agent, Key Eng. Mater. 254–256 (2004) 1045–1050.
[17] L.M. Rodriguez-Lorenzo, M. Vallet-Regi, J.M.F. Ferreira, Fabrication of porous hydroxyapatite bodies by a new direct consolidation method: starch consolidation, J. Biomed. Mater. Res. 60 (2002) 232–240.
[18] M. Potoczek, Hydroxyapatite foams produced by gelcasting using agarose, Mater. Lett. 62 (2008) 1055–1057.
[19] A. Ślósarczyk, PL Patent 154957B1, June 30, 1992.
[20] A. Ślósarczyk, E. Stobierska, Z. Paszkiewicz, M. Gawlicki, Calcium phosphate materials prepared from precipitates with various calcium: phosphorus molar ratios, J. Am. Ceram. Soc. 79 (10) (1996) 2539–2544.
[21] M. Potoczek, Gelcasting of alumina foams using agarose solutions, Ceram. Int. 34 (2008) 661–667.
[22] K.A. Hing, B. Annaz, S. Saeed, P.A. Revell, T. Buckland, Microporosity enhances bioactivity of synthesis bone graft substitutes, J. Mater. Sci. Mater. Med. 16 (5) (2005) 467–475.
[23] A. Bignon, J. Chouteau, J. Chewalier, G. Fantozzi, J.P. Carret, P. Chevassieux, G. Boivin, M. Melin, D. Hartmann, Effect of micro- and macroporosity of bone substitutes on their mechanical properties and cellular response, J. Mater. Sci. Mater. Med. 14 (2003) 1089–1097.
[24] X. Miao, D.M. Tan, J.L. Li, Y. Xiao, R. Crawford, Mechanical and biological properties of hydroxyapatite/tricalcium phosphate scaffolds coated with poly(lactid-co-glycolic acid), Acta Biomater. 4 (2008) 638–645.
[25] L.J. Gibson, M.F. Ashby, Cellular Solids: Structure and Properties, 2nd ed., Cambridge, UK, 1997, pp. 210–211.